Effect of surface defects and adsorbates on the optical anisotropy of Cu(110)

P. D. Lane,* G. E. Isted, and R. J. Cole
SUPA, School of Physics and Astronomy, University of Edinburgh, Edinburgh EH9 3JZ, United Kingdom
(Received 23 March 2010; revised manuscript received 15 June 2010; published 18 August 2010)

We investigate the effects of defects on the optical response of the Cu(110) surface in the spectral region dominated by transitions between surface states. By modeling the variation of reflection anisotropy spectroscopy (RAS) signal with defect coverage we investigate the length scale over which a defect quenches the 2.1 eV RAS peak. We consider a number of different defect types; adatoms, vacancies, and molecular adsorbates, and find that all quench the RAS signal in this region by similar amounts.

DOI: 10.1103/PhysRevB.82.075416 PACS number(s): 78.68.+m, 78.40.−q, 73.20.At

I. INTRODUCTION

Reflection anisotropy (RA) spectroscopy[1] (RAS), also known as reflection difference spectroscopy, is a nonintrusive optical probe of surfaces, which is sensitive to a wide range of surface phenomena including: surface reconstructions,[2,3] dimer orientations,[3,4] and atomic steps.[5,6] Despite this sensitivity the interpretation of RA spectra is non-trivial and quantitative information is often difficult to obtain. However in this work we attempt such a quantitative approach, analyzing a collection of new and published measurements to investigate the sensitivity of the optical response of the Cu(110) surface to various types of surface defect.

The RA spectrum of the clean and well-ordered Cu(110) surface is shown in Fig. 1(a). The spectrum is dominated by a peak at 2.1 eV, arising primarily from transitions between two surface bands which lie in the *p-s* band gap at the $\bar{Y}$ point of the surface Brillouin zone, one occupied the other unoccupied. Photoemission results indicate that the occupied state lies ~0.4 eV below the Fermi energy, E_F,[7–9] while inverse photoemission spectroscopy (IPES) studies reveal the unoccupied state to be ~1.8 eV above E_F.[10–12] Optical transitions between these states require incident light polarized along the [001] direction, producing anisotropy in the surface optical properties and hence a peak in the RA response of the clean Cu(110) surface.

The peak has been shown to be very sensitive to molecular adsorbates which quench its intensity at a rate much greater than the rate of exposure.[13,14] In principle, surface adatoms and vacancies should also reduce the intensity of the peak but no such effect has been observed during ion bombardment of the Cu(110) surface at temperatures of $T=300$ K or higher.[15,16] On the other hand, a recent IPES study by Heskett *et al.*[17] showed that the ion bombardment of this surface at $T=170$ K causes the destruction of the unoccupied state participating in the surface state transition. Heskett *et al.* attributed this observation to the presence of vacancies on the surface, arguing that a minimum clean defect-free area (of order 10×10 lattice parameters) is required to support this unoccupied state. Meanwhile Sun *et al.*[13] have proposed use of the Poelsema-Comsa formalism,[18] more usually employed in the description of He atom scattering, for modeling the intensity of surface state RAS peaks. In this approach it is assumed that He atoms impinging on the surface in proximity to a defect are diffusely scattered. As defect coverage rises, these defect "footprints" overlap increasingly. Neglecting modification of scattering strength by mutual interaction and possible multiple scattering effects, this overlap effect is treated in a geometric fashion: the specular signal is assumed to be proportional to the fraction of surface area which does not fall within the defect footprints. By analogy Sun *et al.*[13] assume that surface state waves are scattered in the same manner, reducing the RAS signal derived from such states. Considering the adsorption of CO on the Cu(110) surface these authors concluded that a single CO molecule could reduce the intensity of the 2.1 eV peak in proportion to an area of order 10^3 Å^2. The two empirical approaches of Refs. 13 and 17 provide alternative algorithms for quantifying the length scale over which surface states lose coherence in the presence of defects, and lead to rather different relations between RAS intensity and defect density.[19] The Heskett model belongs to the discussion of the cluster size needed for a well-formed band structure and is therefore more relevant to the high density regime where only a few isolated clean patches remain while the scattering model used by Sun *et al.*[13] appears better suited to the low-defect density limit. In fact the latter was found to give a good description of the RAS signal of the CO/Cu(110) system throughout the entire concentration range (i.e., from 0 to 1), provided a superposition of three scattering effects was assumed.[13] Applicability of the Poelsema-Comsa formalism to He atom scattering measurements has been extensively verified[18] but very few RAS applications have been reported.[13,19] In this work we provide several more examples by investigating the effects of various physically and chemically distinct defects on the 2.1 eV peak in the RAS spectrum of Cu(110).

II. ION BOMBARDMENT

We consider first the case of ion bombardment of the Cu(110) surface. The experiments were performed in an ultra high vacuum environment with a base pressure of 10^{-10} mbar. The Cu(110) sample was oriented to 0.1° and clean surfaces were prepared by cycles of Argon ion bombardment (500 eV, 1.5 μA/cm^2, 300 K, 15 min) and annealing to 800 K. Atomic order was confirmed by low-energy electron diffraction. The sample could be cooled below room temperature using liquid nitrogen. RA measurements were

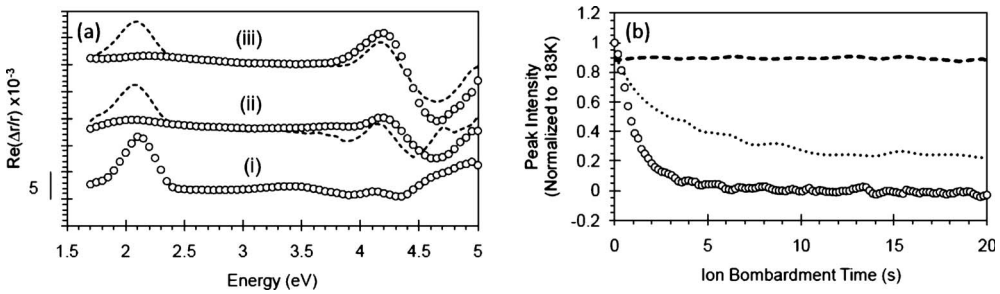

FIG. 1. (a) The RA response of Cu(110) after bombardment at 183 K (open circles) and 303 K (dashed lines) for times of (i) 0 min, (ii) 3 min, and (iii) 21 min. (b) The decay of the RAS signal at 2.1 eV as a function of ion bombardment time for temperatures of 183 K (open circles), 243 K (dotted line), and 303 K (dashed line).

recorded during bombardment with Ar ions with energy of 500 eV and a flux of 1.5 $\mu A/cm^2$.

The circles in Fig. 1(a) show RA results obtained while bombarding the sample at $T=183$ K. The ~4 eV region of the spectra behaves in a similar manner to previous studies at higher temperatures ($T \geq 300$ K) (Refs. 15 and 16) in that the small negative peaks are transformed, on a time scale of order 10^3 s (equivalent to an exposure of ~10 incident ions per surface unit cell), into a large positive peak. However the low-temperature results in Fig. 1(a) differ dramatically from those of earlier studies[15,16] in that we observe a rapid reduction in intensity of the peak at ~2.1 eV; as shown by the circles in Fig. 1(b) the peak is destroyed on a time scale of a few seconds (corresponding to an exposure of order 10^{-2} ions per unit cell). The *shape* of the RAS spectrum in the 2.1 eV region did not appear to change significantly with time. The peak is known to be eroded when molecules are adsorbed on the surface[13,14,20–26] and it appears that the vacancies and adatoms produced by ion bombardment can play the same role.

The dichotomy in 2.1 eV RAS behavior between the high and low-temperature bombardment regimes is emphasized in Fig. 1(b) where we see variation in RAS signal with bombardment time for $T=183$ K (circles), 243 K (dotted line), and 303 K (dashed line). Note that the data is normalized to the 2.1 eV peak intensity at $T=183$ K, and as such the intensity of the peak on the clean surface at higher temperatures is less than 1 due to thermal effects which are discussed in Sec. III. The observed resilience of the 2.1 eV RAS peak under ion bombardment at room temperature shows that the annealing of ion damage is rather efficient at $T=303$ K, for the ion flux used here at least. Below room temperature the 2.1 eV RAS trace indicates incomplete annealing, and we find that the rate of decay of this signal does not vary with temperature below ~220 K. Though beyond the scope of the present work, we note that the temperature dependence of the RAS traces in Fig. 1(b) could in principle reveal the activation barrier for the annealing process. However an understanding of the effect of defects on the RAS signal is a prerequisite to any such analysis. Therefore we concentrate here on the measurements made at 183 K, where the self-annealing process appears to be frozen out and it is reasonable to assume the ion induced defects are effectively immobile and randomly distributed.

To implement the Poelsema-Comsa scattering model[18] numerically we considered a model square lattice consisting of 10^6 sites. For a given defect concentration, c, the appropriate number of defects was randomly distributed on the lattice, each site having an equal probability of becoming the defect site. The RAS signal was then assumed to be destroyed over a square patch of size $N \times N$ lattice parameters centered on each defect site. Equivalently, a site contributes to the RAS signal only if it lies at the center of a clean $N \times N$ patch. Results of simulations performed for several values of N are shown in Fig. 2. These results are essentially indistinguishable from the analytical lattice gas form of the Poelsema-Comsa model but the numerical approach adopted here is readily generalized. Although we present here results for a square lattice and a square scattering patch for ease of discussion, the particular lattice geometry was found to be unimportant.

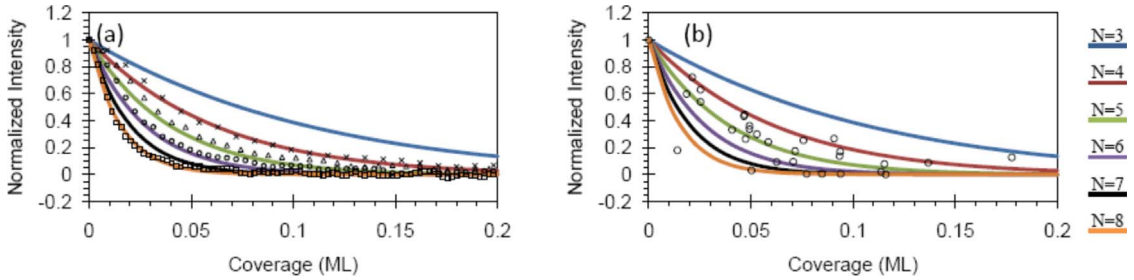

FIG. 2. (Color online) Comparison of Poelsema-Comsa intensity vs coverage curves (solid lines) for patch sizes $N=3$ (blue), $N=4$ (red), $N=5$ (green), $N=6$ (purple), $N=7$ (black), and $N=8$ (orange) with (a): the normalized 2.1 eV RAS intensity, and (b): the IPES data of Heskett *et al.* (Ref. 17). Experimental defect coverages have been determined assuming $Y=1$ (squares), $Y=2$ (circles), $Y=3$ (triangles), and $Y=4$ (crosses).

To map our experimental RAS data onto these simulated curves it is necessary to convert the time axis in Fig. 1(a) to defect concentration, c. In the low coverage regime we can use the expression

$$c = \frac{IYt}{10^{15}}, \tag{1}$$

where I is the number of incident ions per cm^2 per second, Y is the sputter yield (the number of defects created per ion) and t is bombardment time. The symbols plotted in Fig. 2(a) show the results for sputter yields from 1 to 4. The open circles in Fig. 2(b) show the IPES results of Heskett *et al.*[17] who assumed a sputter yield of two defects (vacancies) per ion to calculate coverage. Independent of the assumed value of Y, comparison of the experimental RAS and IPES data provokes two observations. First it is clear that the RAS data in Figs. 1(b) and 2(a) are subject to considerably less noise than is present in Fig. 2(b) for the measurements made with IPES, a considerably more challenging technique. Second, the decay with coverage of the RAS signal is a little faster than that observed with IPES. It can be seen that the simulation for $N=5$ gives a reasonable match to the IPES data from Ref. 17. If we use the same sputter yield as Heskett *et al.* for our RAS data in Fig. 2(a), comparison with the simulations gives $5<N<6$.

The choice of $Y=2$ by Heskett *et al.*[17] is in accord with the literature[27] which suggests that a sputter yield of two vacancies per ion is typical for the ion energies used in Ref. 17 and here. However our previous work[19] has shown that thermally generated adatoms can also destroy the surface state of Ag(110) and, since ion bombardment also generates adatoms, their effect must also be accounted for here. Studies of the adatom yield per ion are limited and it must be estimated in this case. Since ion bombardment is an erosive process we assume a total sputter yield of $Y=3$, corresponding to two vacancies and one adatom. We do not distinguish between the scattering strength of adatoms and vacancies, again exploiting the parallel with He atom scattering for which this assumption has been shown to be valid.[18] From Fig. 2(a) $Y=3$ corresponds to a slightly reduced estimate of the defect footprint to $4<N<5$. Renormalizing the IPES results for $Y=3$ would lead to agreement with the simulation for $N=4$.

III. THERMAL DEFECTS

In contrast to the experimental results for ion bombardment discussed above, where the shape of the RAS spectrum in the 2.1 eV region did not change significantly with defect coverage, the shape of the RA spectrum of the Cu(110) surface is known to evolve somewhat with increasing T. Before considering the attenuation of the RAS intensity by thermally activated defects, it is therefore necessary to first discuss in some detail how the RA spectrum can be simulated.

To account for the thermal behavior of the occupied and unoccupied $\bar{Y}$ surface state bands we adopt the same approach as previous studies.[18,28,29] The parabolic shape of the surface state bands can be described by

$$E(k) = E_0 + \frac{\hbar^2}{2m}|k - k_0|^2, \tag{2}$$

where k is the surface state electron wave vector, $k_0=(0,0.87)$ Å^{-1} (Ref. 28) is the position in reciprocal space of the $\bar{Y}$ point, E_0 are the surface state energies at $\bar{Y}$, and m is the effective mass of the surface state electrons. The experimental value of E_0 for the unoccupied state has been found by inverse photoemission spectroscopy to be 1.8 ± 0.2 eV.[30] While the energy of this state is believed to be independent of temperature,[28,29] photoemission spectroscopy has shown that the occupied state moves toward the Fermi level at a rate of $(2.6\pm0.2)\times10^{-4}$ eV/K with increasing T, taking the value -0.39 ± 0.01 eV at room temperature.[29] The effective masses for the filled and unoccupied surface states are found to be $0.27\pm0.01m_0$ (Ref. 31) and $0.8\pm0.2m_0$,[30] respectively, where m_0 is the mass of a free electron. Integrating over vertical transitions between the surface states in the vicinity of k_0, and accounting for lifetime and Fermi-Dirac broadening, $\Delta\varepsilon_s''$, the imaginary part of the surface dielectric anisotropy arising from the surface state transitions, can be obtained[28,29] from the expression

$$\Delta\varepsilon_s''(\omega,T) \propto \frac{1}{\omega^2}\int_0^\infty L[\omega - E_f(k) + E_i(k),\sigma]F[E_i(k),T]kdk, \tag{3}$$

where E_i and E_f are the initial and final energies of the electronic transition, ω is the photon energy, $L[\omega,\sigma]$ is a Gaussian with width σ, and F is the Fermi-Dirac function accounting for the occupation of the electronic states around E_F. While F has an explicit T dependence, L varies with T on account of the shifting of the occupied surface state energy and the temperature-dependent linewidth $\sigma(T)=(50+0.1\ T)$ meV.[28] The relative importance of each of these effects is discussed in detail in Ref. 32. The complex surface dielectric anisotropy, $\Delta\varepsilon_s$, can be constructed from $\Delta\varepsilon_s''$ using Kramer-Kronig relations, allowing the RA spectrum to be computed

$$\frac{\Delta r}{r}(\omega) \propto \omega\frac{\Delta\varepsilon_s(\omega)}{\varepsilon_b(\omega)-1}, \tag{4}$$

where ε_b is the copper bulk dielectric function obtained from Ref. 33.

Spectra simulated using Eq. (4) for $T=100$ K and 300 K are shown in Fig. 3(a) as dashed and solid curves, respectively. After normalizing Eq. (4) so as to give the correct maximum intensity at 100 K, the calculated curves are seen to provide an excellent reproduction of the corresponding experimental spectra measured by Sun *et al.*[28] (An energy shift of 0.02 eV was applied to the value of E_0 quoted in the previous paragraph for the unoccupied surface state, an amount much smaller than the accuracy to which the energy of this state is known.[30]) The same normalization constant provides good agreement with experiment up to $T\sim400$ K, beyond which Eq. (4) appears to systematically overestimate the integrated area in the 2.1 eV peak, as shown in Fig. 3(b).

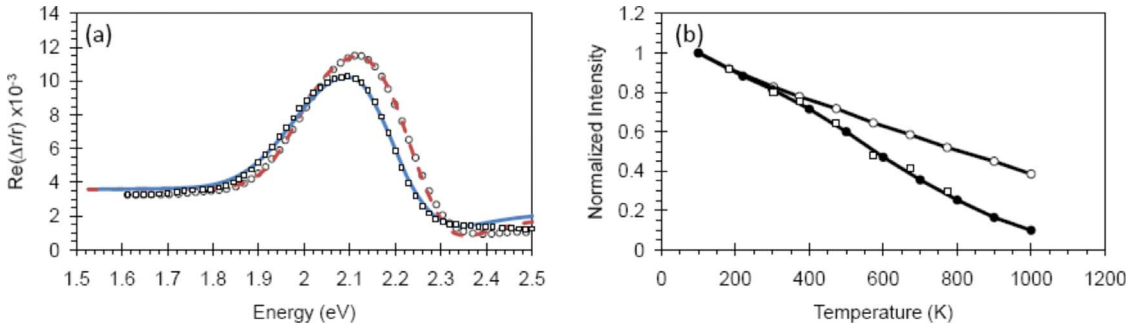

FIG. 3. (Color online) (a) RA spectra of the Cu(110) surface at 100 K (circles) and 300 K (squares) measured by Sun *et al.* (Ref. 28). Spectra simulated using Eq. (4) are also shown for 100 K (dashed line) and 300 K (solid line). The normalization constant in Eq. (4) was chosen so as to reproduce the experimental maximum at 100 K. (b) Integrated intensity in the 2.1 eV peak as a function of temperature calculated from Eq. (4) (open circles) and experimental values from this work (open squares) and of Sun *et al.* (Ref. 28) (filled circles).

A very similar discrepancy was identified in our earlier work[19,32] examining the experimental results of Martin *et al.*[34] for the Ag(110) surface.

In order to account for the difference between the experiment and the simulation we consider the effect of thermal defects. The defect coverage as a function of temperature, $c(T)$ can be calculated using the Arrhenius expression[35]

$$c(T) = \exp\left(\frac{-E_d}{k_B T}\right), \tag{5}$$

where E_d is the defect energy and k_B is Boltzmann's constant. While there are various types and sources of surface defects, most will be derived from the process with lowest energy barrier. We take this to be adatoms "boiling-off" step edges at kink sites onto the terraces where they can disrupt the surface states. Simulated RAS intensities obtained after scaling Eq. (4) according to the Poelsema-Comsa scattering model are shown in Fig. 4 for various values of E_d. It can be seen that the simulations account for the change in slope in the RAS vs T curves observed at ~500 K in the experimental data. Increasing the defect activation barrier has a similar effect on the calculated T dependence of the integrated RAS intensity as increasing the size of the defect footprint. However the best fits to the experimental intensities are obtained with energy barriers in the range $0.2 < E_d < 0.24$ eV, corresponding to a patch size range of $3.5 < N < 5$, as illustrated in Fig. 4(d). Moving away from this range deteriorates the quality of the fit and the experimental data cuts across the simulated curves for more than one patch size, giving rise to the larger error bars in Fig. 4(d). A review of the literature shows that defect activation barriers are difficult to determine with great accuracy, however the range of values we observe is

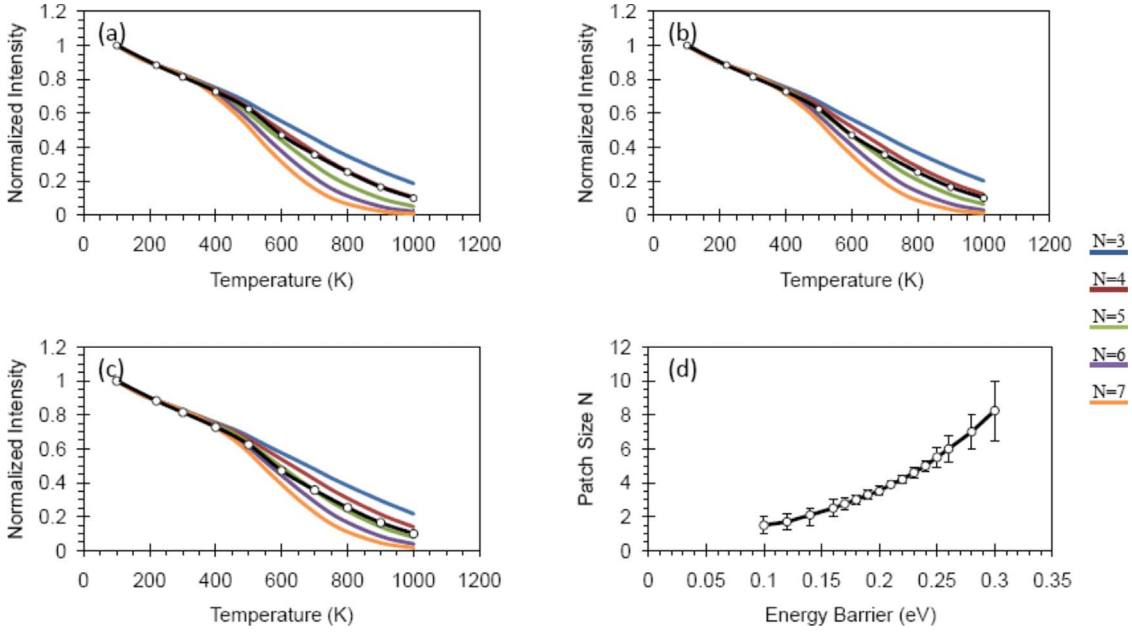

FIG. 4. (Color online) [(a)–(c)] Variation in the normalized intensity of the 2.1 eV peak with temperature. Simulations were performed for patch sizes of $N=3$ (blue), $N=4$ (red), $N=5$ (green), $N=6$ (purple), and $N=7$ (orange), for an adatom formation energy barrier E_d of (a) 0.22 eV, (b) 0.23 eV, and (c) 0.24 eV. In each case the experimental RAS intensities of Sun *et al.* (Ref. 28) are shown as circles. (d) Adatom formation energy barrier against patch size.

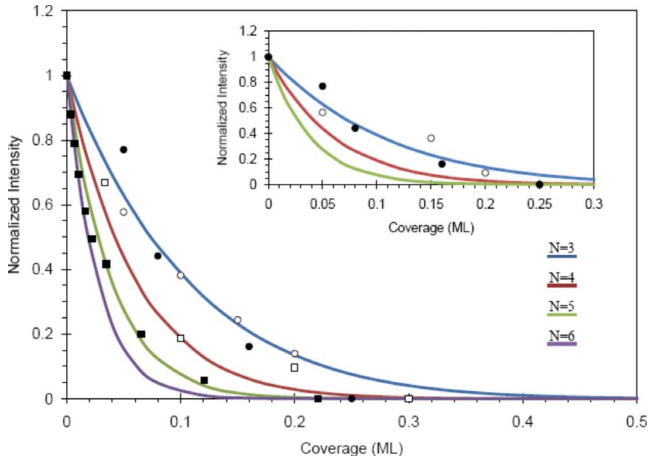

FIG. 5. (Color online) Normalized 2.1 eV peak intensity against adsorbate coverage simulated for patch sizes of $N=3$ (blue), $N=4$ (red), $N=5$ (green), and $N=6$ (purple). Experimental results, derived from integrating the RAS peak, are also shown for silicon (Ref. 14) (open circles), sodium (Ref. 23) (filled circles), methanethiol (Ref. 26) (open squares), and carbon monoxide (Ref. 13) (filled squares) adsorption. Inset shows a comparison of the RAS data (Ref. 22) (filled circles) and IPES data (Ref. 37) (open circles) for the adsorption of sodium.

close to the value reported by Stoltze[36] of 0.24 eV for the formation of an adatom from a kink site on a 001 step.

IV. MOLECULAR ADSORBATES

Progressive decay of the 2.1 eV RAS intensity also occurs when atoms or molecules are adsorbed onto the Cu(110) surface.[13,15,20–26] As noted by Sun *et al.*,[13] such adsorbates can also be considered as surface defects, and hence their effect on the RAS intensity should be amenable to the Poelsema-Comsa patch analysis we have applied to ion-induced and thermally activated surface defects. Experimental results of previous studies using sodium,[23] carbon monoxide,[13] silicon,[14] and methanethiol[26] adsorbates are collected in Fig. 5. Again we define the RAS intensity as the integrated area under the 2.1 eV peak. We use our low temperature ion bombard results as a control to determine the baseline of the peak—we define the surface state as being destroyed when the 2.1 eV region of the spectrum is "flat" [as shown in Fig. 1(a)], thereby rejecting the non-zero optical anisotropy typically exhibited by ordered molecular overlayers at saturation coverage.

Figure 5 compares the patch model to experimental results for sodium,[23] carbon monoxide,[13] silicon,[14] and methanethiol[26] adsorption. For silicon, sodium, and methanethiol, unit coverage is defined as an adsorbate density equal to that of the atomic density of the Cu(110) surface. For CO adsorption, unit coverage corresponds to half this density since each adsorbate occupies a 2×1 unit cell.[13] Although Sun *et al.*[13] considered RAS intensity at 2.13 eV rather than the integral algorithm used here, in the low coverage region ($c<0.05$) we observe in Fig. 5 the same precipitous drop (with a gradient of order −50) with initial CO coverage as that seen in the original paper.[13] However different slopes are observed in the $0.05<c<0.2$ region. This arises because Sun *et al.*[13] renormalize the RAS signal to be 1 at $c=0$ and 0 at $c=1$. On the other hand here we note that the spectrum for $c=0.22$ is flat, resembling that observed after Ar ion bombardment at low temperature, giving a null integral. We attribute the emergence of a negative RAS signal for $c>0.22$ to the growth of a new optical signature characteristic of the ordered CO/Cu(110) monolayer while Sun *et al.*[13] treat this implicitly as a slowly decaying contribution to the intrinsic Cu(110) RAS spectrum.

Despite the different types of molecules used we can see that each appears to reduce the intensity of the surface state by a similar amount with simulations for patch sizes of $N=3$ and $N=6$ bracketing the experimental results. The model may require some refinement when applied to systems using larger molecular adsorbates as effects such as steric hindrance could affect the results.

V. DISCUSSION

While it is pleasing that the role of defects in reducing RAS signals derived from electronic transitions between surface states can be modeled and quantified, it is of fundamental interest to understand its physical origin. In particular it is not clear *a priori* whether the decrease in RAS signal with defect coverage, witnessed in Figs. 1, 3, and 5, is an occupied or unoccupied state effect. A study by Sandl and Bertel[37] shows ultraviolet photoemission spectroscopy (UPS) and IPES results of the occupied and unoccupied states around $\bar{Y}$ for the adsorption of sodium onto the Cu(110) surface; from these results we observe that the unoccupied state is destroyed at a slightly faster rate than the occupied state. In a rigorous binary picture in which the UPS, IPES and RAS signals are destroyed in a region surrounding a defect but unaffected elsewhere, the defect footprint observed in RAS would equal the larger of the IPES and UPS footprints. However a probabilistic interpretation allows defect induced effects on both the occupied and unoccupied surface states to contribute to the RAS footprint, leading to the more general statement: the larger of the UPS and IPES footprints is a lower bound on the footprint observed by RAS. Retreat to a lower bound statement is also motivated by the arguments in Ref. 13. There Sun *et al.*[13] point out that isotropic scattering of the occupied $\bar{Y}$ surface state of Cu(110) could remove the associated optical anisotropy probed by RAS without necessarily quenching the surface state. The comparison between RAS and IPES measurements for the ion bombarded Cu(110) surface (Fig. 2) and for the Na/Cu(110) system (inset of Fig. 5) suggest that the RAS and IPES footprints are similar. Still, given the scatter of the experimental data points, this observation does not rule out a significant role for defect induced destruction of the occupied surface state, or indeed for the depolarization effect proposed by Sun *et al.*[13] Combined RAS, UPS, and IPES studies could reveal the relative importance of defects on the occupied and unoccupied $\bar{Y}$ surface states, and also differentiate between the quenching and depolarization mechanisms.

It should be pointed out that while there is consensus that surface state transitions provide the dominant contribution to the 2.1 eV peak in the RAS spectrum of the Cu(110) surface, it has been suggested that other mechanisms (such as surface-perturbed bulk transitions,[28] surface local field effects,[38,39] and anisotropic intraband effects[28]) also make minor contributions in this spectral region. Although they are not currently understood in sufficient detail, ideally all these effects, and their T dependence, should be accounted for in simulating the RAS spectra. Therefore we must ask two questions: do the experimental results discussed here require us to deduce a "non-surface state" contribution to the Cu(110) RAS spectrum? And how would such contributions modify our analysis and conclusions?

It has been explained in Ref. 28 that measuring the temperature dependence of the Cu(110) RAS spectrum allows investigation of the origins of the optical anisotropy of this surface, and, in principle, facilitates separation of the distinct contributions to it. However we find that the simple surface state calculation, as proposed in Ref. 28 and embodied in Eqs. (3) and (4), gives a rather good description of the *shape* of the experimental spectra measured by the present authors and those of Ref. 28, provided the energy of the unoccupied surface state is fine tuned. This tuning amounts to a shift of 0.02 eV from the exact energy used in Ref. 28 and is an order of magnitude smaller than the quoted experimental uncertainty in its value.[10–12] Given that a number of the remaining parameters required by Eq. (3) [as well as the T dependence of the bulk dielectric function entering Eq. (4)] are also imprecisely known, we feel that the surface state model gives an acceptable description of the shape of the RAS spectra of Cu(110) in the 2.1 eV region. We note that our interpretation of the failure of the surface state model to predict the *intensity* of the experimental RAS signal as the effect of scattering by thermal defects, and our modeling of this effect using the Poelsema-Comsa formalism, leads to an estimate of the defect scattering cross section which is rather similar to that observed for ion-induced defects, together with an estimate of the defect activation barrier consistent with that deduced recently[19] by the same approach for Ag(110) (where the complications mentioned above do not arise).

Although we do not claim here to have unambiguous evidence for non-surface state contributions to the Cu(110) 2.1 eV RAS peak it should be recognized that Sun *et al.*[13] have performed empirical calculations of the optical anisotropy due to surface-modified interband transitions and an anisotropic Drude effect. Using sensible model parameters, these calculations generate broad spectral features in the 2.1 eV region, in part at least due to the presence of the bulk dielectric function in the denominator of Eq. (4). Since it is possible to fit the experimental Cu(110) RAS spectra using a superposition of surface state, surface modified interband transitions and Drude contributions to the surface dielectric anisotropy, $\Delta\varepsilon_s$, the existence of the latter two effects cannot be discounted. The values of N deduced in the present work should therefore be regarded strictly as averages. However the rapid decay of the 2.1 eV RAS signal we observed during low temperature Ar ion bombardment appears to rule out a large contribution which decays linearly with defect coverage: that data could be described satisfactorily with inclusion of a linear contribution with intensity $\leq 10\%$ and with little impact on the results obtained. Differences in data analysis protocols followed here and in Refs. 13 and 28 should not be emphasized. On the contrary we have found the surface state calculation proposed in Ref. 28 and the scattering formalism proposed in Ref. 13 to provide a successful framework for analyzing RAS measurements of a wide variety of modified Cu(110) surfaces, even though we adopted a more conservative interpretation of the experimental data with a correspondingly simpler analysis.

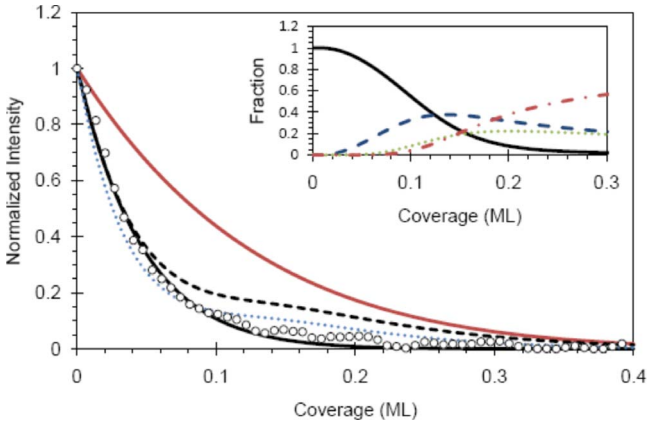

FIG. 6. (Color online) Experimental RAS signal measured during Ar ion bombardment at 183 K (circles). The solid curves show predictions of the Poelsema-Comsa scattering formalism assuming $N=4.6$ and a lattice gas of isolated defects (black line) and a lattice gas of clusters each comprising four defects (red line). Results for a polydispersed mixture of defect clusters are shown for $N=4.6$ (dashed line) and $N=5.2$ (dotted line). The inset shows, for each coverage, the fraction of defects contained in clusters of size 1 (solid line), 2 (dashed line), 3 (dotted line), and 4 (dashed dotted line).

Finally, we consider the validity of the lattice gas assumption employed in our simulations. One might worry, for example, that the positions of defects created at a single Ar ion impact event were correlated, or whether defects (from any impact events) could cluster. Atom scattering measurements for similar systems, comparing sputtering conditions for which $Y=3$ and $Y<1$, have shown[40] that simultaneously created defects are uncorrelated on a length scale of at least four lattice parameters for densities less than 0.04. However these defects were found[40] to diffuse short distances (of order two lattice parameters), even at temperatures below the thermal-diffusion threshold, due to the residual energy delivered to the surface by the ion impact, leading to the growth of small clusters for $c>0.04$. To investigate the effect of clustering we have generalized our numerical scattering calculations to treat the "polydispersed" case, i.e., systems comprising clusters of different sizes. Results are shown in Fig. 6 for a lattice gas of isolated defects (black curve), a lattice gas of defect clusters, all of size 4 (red curve), and a polydispersed system comprising clusters of sizes 1, 2, 3, and 4 (dashed curve). The population of each cluster size was assumed to be coverage dependent in the fashion shown by the inset to Fig. 6. This distribution was created to illustrate qualitatively the

effect of clustering on the RAS signal and was not derived from a realistic description of the surface kinetics. The dashed curve in Fig. 6 shows that the growth of clusters does not modify the initial gradient of the intensity curve but slows the decay of the RAS signal at intermediate defect coverage, as is well known.[18] While $N=4.6$ was used for the solid and dashed curves, the dotted curve in Fig. 6 shows the effect of increasing N to 5.2 for the clustered system. We see that the effect of clustering can be countered by a modest renormalization of N. However the most satisfactory agreement with experiment is achieved in Fig. 6 with $N=4.6$ for a lattice gas of single site defects. Thus in the case of low temperature ion bombardment of Cu(110), it appears that the RAS signal loses most of its intensity before clustering is significant. Similarly, this discussion is not relevant to the case of CO adsorption on Cu(110) studied by Sun *et al.*[13] since this adsorbate is known to form a lattice gas.[41] The potential for clustering to modify our analysis of the effects of thermal defects on RAS signals is hard to estimate. In principle, clustering would lead us to underestimate N for thermal defects and overestimate their formation barrier. Of course each case must be treated on its own merits, but generally we can say that the Poelsema-Comsa scattering model shows greatest defect sensitivity in the low coverage limit, where a lattice gas model would be expected to work best. In principle, the departure of RAS decay from lattice gas behavior at higher coverage should allow interrogation of defect interactions, as is routine in atom scattering.[18]

VI. CONCLUSIONS

We have considered the effects of defects on the surface state contribution to the RAS spectrum of the Cu(110) surface. Despite the consideration of a wide variety of different defects (metallic, covalent, and molecular adsorbates as well as adatoms and vacancies) a consistent picture emerges. We have found that for all the systems considered the coverage dependence of the RAS intensity can be described by the scattering model proposed by Sun *et al.*[13] Furthermore these various defects give rise to rather similarly sized footprints, for a system of isolated defects we find the results lie in the range $3<N<6$.

While good qualitative agreement has been demonstrated between experimental measurements and model simulations, and consistency observed between the effects of various defect types, further detailed investigations of specific cases are warranted. For example, it is desirable to verify the assumed defect yield (i.e., $Y=3$) and distribution (i.e., lattice gas) for the ion damaged surfaces, and in this regard scanning tunneling microscopy would be particularly useful. Similarly combined RAS, IPES, and UPS studies for particular systems would clarify the relative sensitivity of the occupied and unoccupied $\bar{Y}$ surface states to defects, and reveal how these effects combine in optical spectroscopy.

*Corresponding author; plane@staffmail.ed.ac.uk

[1] P. Weightman, D. S. Martin, R. J. Cole, and T. Farrell, Rep. Prog. Phys. **68**, 1251 (2005).
[2] D. E. Aspnes, J. P. Harbison, A. A. Studna, and L. T. Florez, J. Vac. Sci. Technol. A **6**, 1327 (1988).
[3] M. Wassermeier, I. Kamiya, D. E. Aspnes, L. T. Florez, and J. P. Harbison, J. Vac. Sci. Technol. B **9**, 2263 (1991).
[4] J. R. Power, P. Weightman, S. Bose, A. I. Shkrebtii, and R. Del Sole, Phys. Rev. Lett. **80**, 3133 (1998).
[5] J. R. Power, T. Farrell, P. Gerber, S. Chandola, P. Weightman, and J. F. McGilp, Surf. Sci. **372**, 83 (1997).
[6] S. G. Jaloviar, J. L. Lin, F. Liu, V. Zielasek, L. McCaughan, and M. G. Lagally, Phys. Rev. Lett. **82**, 791 (1999).
[7] P. Heimann, J. Hermanson, H. Miosga, and H. Neddermeyer, Surf. Sci. **85**, 263 (1979).
[8] S. Kevan, Phys. Rev. B **28**, 4822 (1983).
[9] P. Straube, F. Pforte, T. Michalke, K. Berge, A. Gerlach, and A. Goldmann, Phys. Rev. B **61**, 14072 (2000).
[10] R. A. Bartynski, T. Gustafsson, and P. Soven, Phys. Rev. B **31**, 4745 (1985).
[11] B. Reihl and K. H. Frank, Phys. Rev. B **31**, 8282 (1985).
[12] R. Schneider, H. Durr, Th. Fauster, and V. Dose, Phys. Rev. B **42**, 1638 (1990).
[13] L. D. Sun, M. Hohage, P. Zeppenfeld, R. E. Balderas-Navarro, and K. Hingerl, Phys. Rev. Lett. **90**, 106104 (2003).
[14] D. S. Martin, J. Phys.: Condens. Matter **21**, 405003 (2009).
[15] J. Bremer, J.-K. Hansen, and O. Hunderi, Surf. Sci. **436**, L735 (1999).
[16] B. F. Macdonald and R. J. Cole, Phys. Status Solidi A **188**, 1489 (2001).
[17] D. Heskett, D. DePietro, G. Sabatino, and M. Tammarro, Surf. Sci. **513**, 405 (2002).
[18] B. Poelsma and G. Cosma, *Scattering of Thermal Energy Atoms*, Springer Tracts in Modern Physics Vol. 115 (Springer, Berlin, 1989).
[19] G. E. Isted, P. D. Lane, and R. J. Cole, Phys. Rev. B **79**, 205424 (2009).
[20] B. G. Frederick, J. R. Power, R. J. Cole, C. C. Perry, Q. Chen, S. Haq, Th. Bertrams, N. V. Richardson, and P. Weightman, Phys. Rev. Lett. **80**, 4490 (1998).
[21] R. J. Cole, B. G. Frederick, J. R. Power, C. C. Perry, Q. Chen, C. Verdozzi, N. V. Richardson, and P. Weightman, Phys. Status Solidi A **170**, 235 (1998).
[22] C. C. Perry, B. G. Frederick, J. R. Power, R. J. Cole, S. Haq, Q. Chen, N. V. Richardson, and P. Weightman, Surf. Sci. **427-428**, 446 (1999).
[23] D. S. Martin, A. M. Davarpanah, S. D. Barrett, and P. Weightman, Phys. Rev. B **62**, 15417 (2000).
[24] N. P. Blanchard, D. S. Martin, A. M. Davarpanah, S. D. Barrett, and P. Weightman, Phys. Status Solidi A **188**, 1505 (2001).
[25] L. D. Sun, M. Hohage, and P. Zeppenfeld, Phys. Rev. B **69**, 045407 (2004).
[26] D. S. Martin, P. D. Lane, G. E. Isted, R. J. Cole, and N. P. Blanchard, Phys. Rev. B (to be published).
[27] V. S. Smentkowski, Prog. Surf. Sci. **64**, 1 (2000).
[28] L. D. Sun, M. Hohage, P. Zeppenfeld, and R. E. Balderas-

Navarro, Surf. Sci. **589**, 153 (2005).
[29] A. Gerlach, G. Meister, R. Matzdorf, and A. Goldmann, Surf. Sci. **443**, 221 (1999).
[30] A. Goldmann, V. Dose, and G. Borstel, Phys. Rev. B **32**, 1971 (1985).
[31] S. D. Kevan, N. G. Stoffel, and N. V. Smith, Phys. Rev. B **31**, 3348 (1985).
[32] G. E. Isted, P. D. Lane, and R. J. Cole, Phys. Status Solidi B **247**, 1965 (2010).
[33] D. W. Lynch and W. R. Hunter, in *Handbook of Optical Constants of Solids*, edited by E. D. Palik (Academic, Orlando, London, 1985).
[34] D. S. Martin, N. P. Blanchard, P. Weightman, D. S. Roseburgh, R. J. Cole, J.-K. Hansen, J. Bremer, and O. Hunderi, Phys. Rev. B **76**, 115403 (2007).
[35] R. M. Tromp and M. Mankos, Phys. Rev. Lett. **81**, 1050 (1998).
[36] P. Stoltze, J. Phys.: Condens. Matter **6**, 9495 (1994).
[37] P. Sandl and E. Bertel, Surf. Sci. **302**, L325 (1994).
[38] J.-K. Hansen, J. Bremer, and O. Hunderi, Surf. Sci. Lett. **418**, L58 (1998).
[39] J.-K. Hansen, J. Bremer, and O. Hunderi, Phys. Status Solidi A **170**, 271 (1998).
[40] B. Poelsema, K. Lenz, L. S. Brown, L. K. Verheij, and G. Comsa, Surf. Sci. **162**, 1011 (1985).
[41] M. Kunat, Ch Boas, Th Becker, U. Burghas and Wöll, Surf. Sci. **474**, 114 (2001).